Induction and relaxation of optical second-order nonlinearity in tellurite glasses

Aiko Narazaki, Katsuhisa Tanaka, Kazuyuki Hirao, and Naohiro Soga
Department of Material Chemistry, Graduate School of Engineering, Kyoto University, Sakyo-ku, Kyoto 606-8501, Japan

(Received 29 May 1998; accepted for publication 12 November 1998)

Second harmonic generation has been examined for $30ZnO \cdot 70TeO_2$ glass with a two-step poling procedure in order to understand the poling temperature dependence of second harmonic intensity. When the poling temperature increases, the second harmonic intensity increases, manifests a maximum at the temperature which we call an optimum poling temperature, and decreases drastically just below the glass transition temperature. The glass treated with two-step poling, which includes poling at 300 °C and subsequent poling at the optimum poling temperature, i.e., 280 °C, exhibits much smaller second harmonic intensity and more unambiguous Maker fringe pattern than that poled only at 280 °C. This fact suggests that the decrease in second harmonic intensity with an increase in poling temperature cannot be attributed to a reversible process like a thermal fluctuation of dipoles, but is governed by an irreversible one. Based on a linear relation between the optimum poling temperature and glass transition temperature, the irreversible process is deduced to consist of some oxidation reactions such as a migration of nonbridging oxide ions to and subsequent evaporation of oxygen gas at the anode side. Decay of the second harmonic intensity for $30NaO_{1/2} \cdot 70TeO_2$ glass as well as $30ZnO \cdot 70TeO_2$ glass has also been examined at room temperature. Whereas the $30ZnO \cdot 70TeO_2$ glass does not show a decay, the second harmonic intensity of the $30NaO_{1/2} \cdot 70TeO_2$ glass decays rapidly with an average relaxation time of 10 h. This relaxation behavior is explainable in terms of the difference in mobility between Zn^{2+} and Na^{+} ions. © *1999 American Institute of Physics.* [S0021-8979(99)04704-0]

I. INTRODUCTION

Optical second-order nonlinearity observed in poled glass materials is a subject of great interest from both fundamental and practical standpoints. The fundamental interest finds its origin in the fact that a disappearance of inversion symmetry is induced in a disordered system such as glass and is frozen even after a high voltage is removed. From a practical viewpoint, the poled glasses will be useful as a frequency doubler of light and a linear electro-optical device. Since the discovery of second harmonic generation in poled silica glass by Myers *et al.*,[1] the silica-based glasses have been investigated most extensively.[2–8] Tellurite glass is also known to exhibit second harmonic generation when the thermal poling is carried out.[9–15] A peculiar point of tellurite glass is its low glass transition temperature, which is very close to the poling temperature. This fact enables us to analyze in detail a change of glass structure in the vicinity of the glass transition temperature under an applied high voltage. Recently, we reported poling temperature dependence of second harmonic intensity for $MgO–ZnO–TeO_2$,[12,13] $Na_2O–ZnO–TeO_2$,[14] and $Li_2O–Na_2O–TeO_2$[15] glass systems. With an increase in poling temperature, the second harmonic intensity increases, takes a maximum value, and decreases. It was also found that the poling temperature corresponding to the highest second harmonic intensity, which we referred to as an optimum poling temperature in our previous paper, is proportional to the glass transition temperature. The close relation between the optimum poling temperature and the glass transition temperature leads to such a possible mechanism that the tellurite glass network structure containing nonbridging oxygens with negative charge takes part in a process which decreases the second harmonic intensity in the vicinity of the glass transition temperature.

In the present work, we examined the second harmonic generation in $30ZnO \cdot 70TeO_2$ glass with a two-step poling procedure to investigate in detail the cause for the decrease in second harmonic intensity just below the glass transition temperature. The two-step poling procedure gives us a new sight for the induction mechanism of second harmonic generation. We also report the relaxation behavior of second harmonic intensity at room temperature in $30ZnO \cdot 70TeO_2$ and $30NaO_{1/2} \cdot 70TeO_2$ glasses, and discuss the difference in relaxation behavior between these two systems in the light of the diffusion ability of Na^{+} and Zn^{2+} ions.

II. EXPERIMENTAL PROCEDURE

A. Sample preparation

Glass samples were prepared from ZnO, Na_2CO_3, and TeO_2. The purity of these raw materials was 99%, 99.5%, and 99%. The powders of the raw materials were mixed thoroughly to make $30ZnO \cdot 70TeO_2$ and $30NaO_{1/2} \cdot 70TeO_2$ compositions and melted in a platinum crucible at 850–900 °C for 20 min in air. The melt was rapidly cooled by pouring onto an alumina plate to obtain glass. The glass transition temperature was measured using differential thermal analysis (Rigaku, TG-DTA8112BH). After the glass was an-

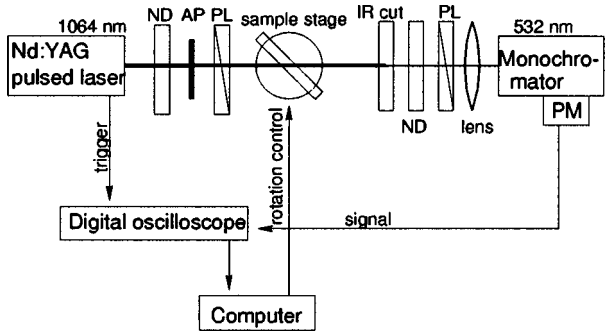

FIG. 1. Schematic illustration of equipment for second harmonic generation measurements. The second harmonic wave is detected with a photomultiplier tube after the elimination of fundamental wave by using an IR cut filter and a monochromator. The meanings of abbreviations are as follows. ND: ND filter; AP: aperture; PL: polarizer; IR cut: IR cut filter; and PM: photomultiplier.

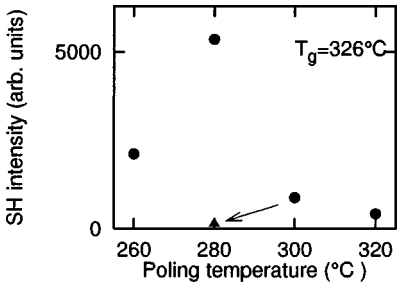

FIG. 2. Poling temperature dependence of second harmonic intensity for $30ZnO \cdot 70TeO_2$ glass. The closed circles correspond to the intensity for glasses poled at each of the temperatures for 20 min. The closed triangle represents the intensity for the glass after two-step poling; the sample was finally poled at 280 °C for 20 min after the initial poling at 300 °C for 20 min.

nealed at around the glass transition temperature for 20 min, it was cut into a plate. Both surfaces of the plate-like glass were polished for measurements of second harmonic generation. The resultant glass specimen had a thickness of 1 mm.

Poling of the glass sample was performed as follows. The glass sample was sandwiched in between two commercial borosilicate glass plates with a thickness of 0.15 mm and contacted physically with electrodes made of stainless steel. The commercial borosilicate glass plates were used to avoid precipitation of metallic tellurium which occurred on the cathode-side glass surface when the glass sample was directly brought into contact with the electrodes made of stainless steel.[13] The use of commercial borosilicate glass plates was also effective to avoid discharge between the electrodes. The glass sample sandwiched with the electrodes was put into an electric furnace and held at an aimed temperature for 30 min. After the voltage of 3 kV was applied for 20 min at the temperature, the glass sample was taken out from the furnace and kept at room temperature for 60 min with the constant voltage applied. In addition to the above-described poling, we carried out two-step poling treatment for the $30ZnO \cdot 70TeO_2$ glass. Under the constant voltage of 3 kV, the glass sample was heated at 300 °C for 20 min in the first step and succeedingly heated at 280 °C for 20 min in the second step. Then, it was quenched to the room temperature with the voltage being kept constant. It should be noted that the actual voltage applied to the glass sample was less than 3 kV because of the use of borosilicate glass plates. The actual voltage applied to the sample was estimated to be 1.7 kV, when the dielectric constants of $30ZnO \cdot 70TeO_2$ and borosilicate glasses were assumed to be 21 (Ref. 16) and 7.9 (Ref. 17), respectively.

B. Optical measurements

Second harmonic generation of the poled glass samples was measured using the Maker fringe method with a setup illustrated in Fig. 1. A pulsed Nd:YAG laser (Spectra Physics, GCR-11), which operated in a *Q*-switched mode with a 10 Hz repetition rate, was used as a light source. After the pulse at 1064 nm with 9 ns duration was *p* polarized, it was incident on the sample at $-65°$ to 65°. The beam diameter was about 1 mm. The output light from the poled glass sample was passed through both an IR cut filter and a monochromator (Spex, 270M) to completely eliminate the fundamental wave at 1064 nm. The second harmonic wave at 532 nm thus obtained was detected with a photomultiplier (Hamamatu Photonics, R955). The signal from the photomultiplier was integrated by using a digital oscilloscope (Hewlett Packard 54522A). The second harmonic intensity from a Y-cut quartz with a thickness of 1.046 mm and $d_{11} = 0.34$ pm/V was also measured for the purpose of determining input light power and calculating second-order nonlinear optical coefficient of the samples.

Refractive indices at 532 and 1064 nm were measured using an ellipsometer (Yokojiri, DVA-36VW) for the $30ZnO \cdot 70TeO_2$ glass poled at 280 °C to estimate second-order nonlinear optical coefficient.

III. RESULTS

Figure 2 shows the dependence of second harmonic intensity on poling temperature for $30ZnO \cdot 70TeO_2$ glass with an accuracy of $\pm 10\%$. The closed circles denote the second harmonic intensity for the glasses poled at the specified temperatures for 20 min, whereas the closed triangle represents the intensity for the glass treated with two-step poling procedure. As found from the results of one-step poling (closed circles), a maximum clearly appears at 280 °C, which corresponds to an optimum poling temperature.[12] The second harmonic intensity for the glass poled in two steps is almost the same as the intensity obtained for the glass poled at 300 °C, and much lower than that for the glass poled at the optimum poling temperature equal to 280 °C. Namely, the change to cause the decrease in second harmonic intensity just below the glass transition temperature is an irreversible process.

The variation of second harmonic intensity with angle of incidence for $30ZnO \cdot 70TeO_2$ glasses poled in two steps and in single step at 280 °C is shown by using solid curves in Figs. 3(a) and 4, respectively. According to the Maker fringe theory,[18,19] the second harmonic intensity $P_{2\omega}$ can be expressed by the following equations:

$$P_{2\omega} = C d_{\mathrm{eff}}^2 t_\omega^4 T_{2\omega} R(\theta) P_\omega^2 [1/(n_\omega^2 - n_{2\omega}^2)^2] \sin^2 \Psi, \quad (1)$$

$$\Psi = (2\pi L/\lambda)(n_\omega \cos\theta_\omega - n_{2\omega} \cos\theta_{2\omega}), \quad (2)$$

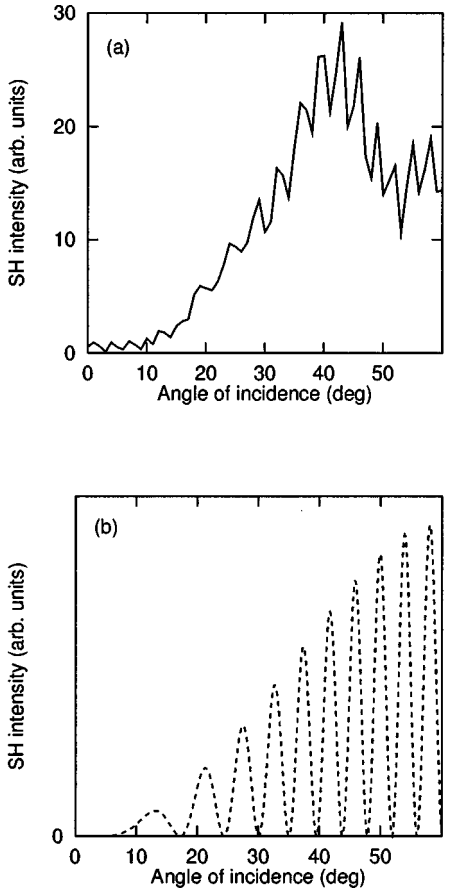

FIG. 3. (a) Experimental Maker fringe pattern of $30ZnO \cdot 70TeO_2$ glass poled in two steps, (b) theoretical Maker fringe pattern drawn by using Eqs. (1)–(3) with $L=1$ mm, $n_{2\omega}=2.05$, and $n_{\omega}=2.00$.

where C is a constant, t_{ω} and $T_{2\omega}$ are the transmission factors, $R(\theta)$ is the multiple reflection correction, P_{ω} is the fundamental power, n_{ω} and $n_{2\omega}$ are the refractive indices, θ_{ω} and $\theta_{2\omega}$ are the refraction angles. Here, subscripts ω and 2ω mean fundamental and second harmonic waves, respectively. The effective second-order nonlinear coefficient d_{eff} is written by Eq. (3), if we assume that the Kleinman symmetry is satisfied and that the electric dipoles are isotropic, oriented perpendicular to the sample surface with $C_{\infty v}$ symmetry, and uniformly distributed over the thickness L:

$$d_{\text{eff}}=\tfrac{2}{3}d_{33}\sin\theta_{\omega}\cos\theta_{\omega}\cos\theta_{2\omega}+(\tfrac{1}{3}d_{33}\cos^2\theta_{\omega}+d_{33}\sin^2\theta_{\omega})\sin\theta_{2\omega}. \quad (3)$$

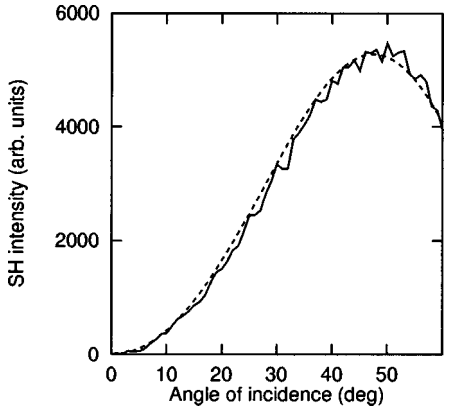

FIG. 4. Maker fringe patterns for $30ZnO \cdot 70TeO_2$ glass poled at 280 °C with 3 kV. The solid and broken curves denote the experimental and theoretical patterns, respectively. The theoretical curve was drawn with $d_{33}=0.45$ pm/V, $L=27$ μm, $n_{2\omega}=2.05$ and $n_{\omega}=2.00$.

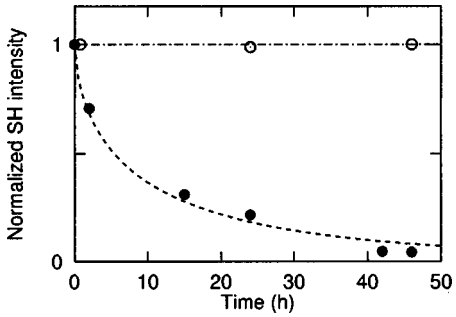

FIG. 5. Relaxation behavior of second harmonic intensity for $30ZnO \cdot 70TeO_2$ (open circles) and $30NaO_{1/2} \cdot 70TeO_2$ (closed circles) glasses. The broken curve was drawn by using Eq. (4) with $\tau=10$ h and $\beta=0.6$. For $30ZnO \cdot 70TeO_2$ glass, the intensity does not decay in a few weeks and shows more than 90% of its initial intensity even after one year. It should be noted that the initial intensity of $30ZnO \cdot 70TeO_2$ glass is about fifty times larger than for $30NaO_{1/2} \cdot 70TeO_2$ glass.

The broken curve in Fig. 3(b) graphically represents the theoretical Maker fringe pattern drawn by using Eqs. (1)–(3) on the assumption that $L=1$ mm, which corresponds to the glass sample thickness, $n_{\omega}=2.00$ and $n_{2\omega}=2.05$. Although the theoretical pattern is in accordance with the experimental one regarding the spacing between minima, the theoretical intensity at the minima is different from the experimental one; the former is zero while the latter shows non-zero values. The Maker fringe pattern such as the experimental fringe in Fig. 3(a) is obtained if the second harmonic waves with different amplitude are generated from surface layers of the glass which are separated by about 1 mm and interfere with each other. By contrast, the experimental fringe in Fig. 4 which exhibits a minimum only at the incident angle of 0° indicates that the second harmonic waves are produced only in a thin layer with a thickness around the coherence length $\simeq 5$ μm. Moreover, this thin layer was found to be near the glass surface which had been contacted with the anode during poling because the second harmonic generation was not observed when the anode-side surface with about 30 μm was etched mechanically. The application of Eqs. (1)–(3) with $L=27$ μm and $d_{33}=0.45$ pm/V, which is indicated by the broken curve in Fig. 4, results in a good agreement with the experimental pattern.

Figure 5 shows the variation of second harmonic intensity with time after the high voltage was removed. The open and closed circles represent the intensity for $30ZnO \cdot 70TeO_2$ glass poled at 280 °C and $30NaO_{1/2} \cdot 70TeO_2$ glass poled at 220 °C, respectively. For $30NaO_{1/2} \cdot 70TeO_2$ glass, the optimum poling temperature is 225 °C, which is about 30 °C below the glass transition temperature. The second harmonic intensity of the $30ZnO \cdot 70TeO_2$ glass does not decay in a

few weeks. On the contrary, the intensity keeps more than 90% of its initial value even after one year. In contrast, a decay of second harmonic intensity was observed in the $30NaO_{1/2}\cdot 70TeO_2$ glass. The average relaxation time τ was determined by fitting the following function $f(t)$ to the experimental data indicated by the closed circles:

$$f(t)=\exp\left[-\left(\frac{t}{\tau}\right)^{\beta}\right], \tag{4}$$

which is generally used for the purpose of analyzing nonexponential relaxation behavior. The broken curve was drawn on the assumption that $\tau=10$ h and $\beta=0.6$. The agreement between experimental data and the theoretical curve is rather good. It is concluded that the average relaxation time for the decay of second harmonic intensity is about 10 h in the case of $30NaO_{1/2}\cdot 70TeO_2$ glass. The value of β less than 1 means that the relaxation time has a rather broad distribution. The same analysis was recently performed by Qiu *et al.*[20] for soda lime silicate glass.

IV. DISCUSSION

In general, the application of high voltage at high temperatures to glass containing mobile cations causes a migration of cations toward a cathode, resulting in a formation of depletion region and a pile of the cations beneath the anode- and cathode-side glass surfaces, respectively. The depletion region is likely to develop to greater extent if the mobility of cations is much larger than that of nonbridging oxide ions. Carlson reported that Na^+ ion-depleted layer was formed over about 1 μm below the anode-side glass surface when $20Na_2O\cdot 80SiO_2$ (wt %) glass was heated with 100 V for 2.5 h at 475 °C.[21] Moreover, the pile of mobile cations was observed in the thin layer near the anode.[22] Such a pile of cations can be explained as follows. In the depletion region a large net negative charge is left. The cations are attracted to the depletion region by the large Coulomb force. Then, this Coulomb force is able to balance with the opposite external electric force, making the pile of cations near the anode.

Similarly, when the poling is performed for $30ZnO\cdot 70TeO_2$ and $30NaO_{1/2}\cdot 70TeO_2$ glasses, a thin layer with Zn^{2+} and Na^+ ions depleted is thought to be developed near the anode-side surface to which the major part of the external electric field is applied. The depletion layer has a space charge composed of nonbridging oxygens. A pair of separated charges with opposite signs, namely nonbridging oxygen in the depletion layer and cation accumulated near the anode, creates an electric field in the opposite direction of the external electric field. Thus, the thermal poling of tellurite glasses produces a strong electric field in the thin layer beneath the anode and breaks the macroscopic inversion symmetry of the glass structure. This frozen electric field E_{dc} in the glass induces the observable second-order nonlinear susceptibility $\chi^{(2)}$ via both an orientation of nonbridging oxide ions in the depleted region and the third-order nonlinear effect, i.e., $\chi^{(3)}\ E_{dc}$. We estimated the magnitude of $\chi^{(2)}=\chi^{(3)}\ E_{dc}$ for $30ZnO\cdot 70TeO_2$ glass as follows. When the poling is carried out at 280 °C, the actual voltage of 1.7 kV is approximately applied to the thickness of $L=27$ μm near the anode, leading to being that E_{dc} is about 6×10^7 V/m. Therefore, using $\chi^{(3)}=1.10\times 10^{-20}\,m^2/V^2$ reported by Berthereau *et al.*,[23] $\chi^{(2)}$ can be calculated as 0.7 pm/V. The magnitude of estimated $\chi^{(2)}$ is comparable to the value obtained experimentally, i.e., $\chi^{(2)}=0.90$ pm/V.

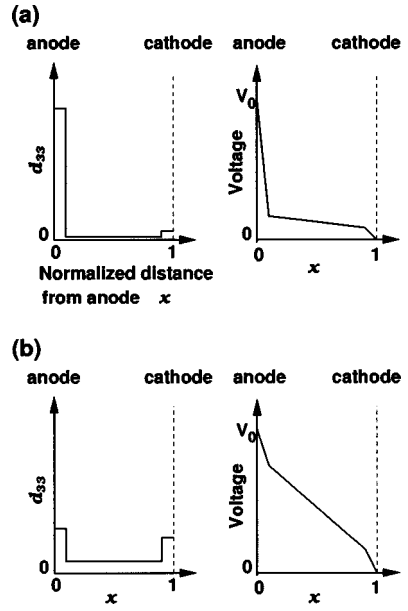

FIG. 6. Schematic diagrams for variation of second-order nonlinear optical coefficient d_{33} and applied voltage with normalized distance from anode-side glass surface x for the $30ZnO\cdot 70TeO_2$ glass poled by (a) single-step and (b) two-step processes.

The poling temperature dependence of second harmonic intensity indicated by closed circles in Fig. 2 has been commonly observed in $MgO–ZnO–TeO_2$, $Na_2O–ZnO–TeO_2$, and $Li_2O–Na_2O–TeO_2$ glass systems. Up to the optimum poling temperature, i.e., 280 °C, the second harmonic intensity increases with an increase in poling temperature. Based upon the above-described mechanism of induction of second harmonic generation, such an increase in the intensity is attributed to an augmentation in easiness to form the internal dc electric field. At higher temperatures, the depletion of cations is more readily promoted near the anode-side surface.[24] Consequently, the larger internal electric field and the larger second harmonic generation are induced. In fact, Proctor and Sutton revealed experimentally that the development of voltage which dropped near the anode electrode occurred more drastically at higher temperature for lead borosilicate glass.[25] The Maker fringe pattern shown in Fig. 4 is also explainable considering the previous mechanism that an origin of the second harmonic generation exists only in a thin layer beneath the anode-side glass surface. This situation is schematically presented in Fig. 6(a), where a distribution of d_{33} as well as electric field is illustrated.

On the other hand, the fact that second harmonic intensity decreases just below the glass transition temperature cannot be explained under the above-described model which assumes the mobile cations and immobile nonbridging oxide ions, and needs consideration that the change in behavior of both cations and nonbridging oxide ions. The linear relation between optimum poling temperature and glass transition

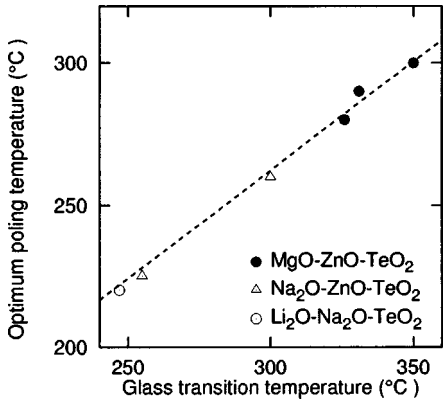

FIG. 7. Relation between optimum poling temperature and glass transition temperature observed in $MgO–ZnO–TeO_2$ (closed circles), $Na_2O–ZnO–TeO_2$ (open triangles), and $Li_2O–Na_2O–TeO_2$ (open circle) glass systems. The broken line was drawn by the method of least squares.

temperature shown in Fig. 7 supports an idea that the decrease in second harmonic intensity results from the viscous flow of glass network structure, which includes an increase in mobility of nonbridging oxygens. On a plausible assumption that the viscous flow plays an important role in the decrease in second harmonic intensity, we previously suggested two possible mechanisms to reduce the second harmonic intensity as follows. One of them includes the conduction of nonbridging oxide ions toward an anode side and subsequent evaporation into the air in the form of O_2, which decreases the internal electric field in the depletion layer.[21] The oxidation reaction to change the valence of Te^{4+}, which reduces the negative charge in the depletion region, is also possible. In another mechanism, when the poling temperature approaches the glass transition temperature, the nonbridging oxygens begin to vibrate more vigorously, leading to a thermal fluctuation of electric dipoles and a reduction in orientation. Whether it is more reasonable is clear from the experiments of the two-step poling process. In the latter case, the internal electric field does not change so that the orientation of dipoles and second harmonic intensity should recover if the poling is performed again at the optimum poling temperature after the initial poling at higher temperature. In contrast, since the former mechanism includes an irreversible electrochemical reaction such as the evaporation, the second poling process at the optimum poling temperature does not bring about an increase in second harmonic intensity. The result shown in Fig. 2 clearly indicates that the decrease in second harmonic intensity occurs irreversibly just below the glass transition temperature. Thus, the former mechanism is more plausible, although further experiments are required to determine what kinds of electrochemical reactions are predominant.

At the top of this section, we described that the dipole moment along the external electric field is induced in the thin depletion layer near the anode-side surface. Nevertheless, the profile of Maker fringe pattern such as Fig. 3(a) suggests the presence of more than two layers, which are separated with each other by the sample thickness and generate second harmonic waves with different amplitude. This profile of Maker fringe pattern is generally observed in the tellurite glass with low second harmonic intensity such as the glass poled at a temperature close to the glass transition temperature. In support of this observation, we conclude that the decrease in space charge in the depletion layer beneath the anode-side glass surface leads to a lesser voltage drop near the anode side, resulting in such a situation that the external electric field is likely applied to the whole bulk glass and second-order nonlinearity is induced in other regions than the anode-side glass surface, as shown in Fig. 6(b).

The second harmonic intensity of $30ZnO \cdot 70TeO_2$ glass did not decay in a few weeks but lasts more than one year, whereas a rapid relaxation of intensity was observed at room temperature for $30NaO_{1/2} \cdot 70TeO_2$ glass, as demonstrated in Fig. 5. It is reasonable to argue that in oxide glasses alkali ions diffuse more easily than divalent cations, because the alkali ion is approximately bonded to only one nonbridging oxygen and needs less energy to break the bond to diffuse. In the $Na_2O \cdot 9SiO_2$ glass, for example, self-diffusion coefficient of sodium ions D^*_{Na} is $\sim 10^{-12}\,cm^2/s$ at 210 °C, whereas that of calcium ions D^*_{Ca} is $\sim 10^{-16}\,cm^2/s$ at 450 °C.[26] Therefore, the rapid relaxation of second harmonic intensity in the $30NaO_{1/2} \cdot 70TeO_2$ glass is ascribable to the diffusion of sodium ions caused by the concentration gradient which was made during the poling. Considering this fact, a glass containing a large amount of alkali ions is not suitable for an application to devices, and it is necessary to choose glass composition containing relatively mobile divalent cations with small size such as Zn^{2+} ions for the purpose of realizing a long-lasting polarization.

V. CONCLUSIONS

It is known for various tellurite glasses that with an increase in poling temperature, the second harmonic intensity increases, manifests a maximum at the temperature which we call the optimum poling temperature, and then decreases. In the present work, the second harmonic intensity was measured for $30ZnO \cdot 70TeO_2$ glass after two-step poling procedure; the glass was first poled at 300 °C and succeedingly poled at 280 °C corresponding to its optimum poling temperature. Because the second harmonic intensity did not recover the maximum value obtained by single-step poling at 280 °C, it is concluded that the decrease in second harmonic intensity occurred irreversibly just below the glass transition temperature. In order to interpret this result, we suggest a mechanism to induce and to reduce the second harmonic generation as follows. Up to the optimum poling temperature, the formation of a thin depleted layer of mobile cations beneath the anode and the subsequent orientation of nonbridging oxygens in the depletion layer produce the strong electric field in the opposite direction of the external field, leading to the second harmonic generation. On the other hand, in the vicinity of the glass transition temperature, some oxidation reactions such as $O^{2-} \rightarrow \frac{1}{2}O_2 + 2e^-$ and $Te^{4+} \rightarrow Te^{6+} + 2e^-$, which reduce the internal electric field, presumably take place. We also found that the second harmonic intensity of $30ZnO \cdot 70TeO_2$ glass kept its initial value at room temperature while the intensity decayed with an av-

erage relaxation time of 10 h for $30NaO_{1/2}\cdot 70TeO_2$ glass. The latter phenomenon is attributed to the larger diffusion coefficient of sodium ions compared with divalent zinc ions.

ACKNOWLEDGMENT

The authors would like to thank Professor T. Yoko of Institute for Chemical Research, Kyoto University, for the measurements of refractive index.

[1] R. A. Myers, N. Mukherjee, and S. R. J. Brueck, Opt. Lett. **16**, 1732 (1991).
[2] H. Nasu, H. Okamoto, A. Mito, J. Matsuoka, and K. Kamiya, Jpn. J. Appl. Phys., Part 2 **32**, L406 (1993).
[3] J. M. Dell, M. J. Joyce, and G. O. Stone, Proc. SPIE **2289**, 185 (1994).
[4] P. G. Kazansky, L. Dong, and P. S. J. Russell, Electron. Lett. **30**, 1345 (1994).
[5] K. Tanaka, K. Kashima, K. Hirao, N. Soga, S. Yamagata, A. Mito, and H. Nasu, Jpn. J. Appl. Phys., Part 1 **34**, 175 (1995).
[6] T. Fujiwara, D. Wong, Y. Zhao, S. Fleming, S. Poole, and M. Sceats, Electron. Lett. **31**, 573 (1995).
[7] H. Takebe, P. G. Kazansky, and P. S. J. Russell, Opt. Lett. **21**, 468 (1996).
[8] H. Imai, S. Horinouchi, Y. Uchida, H. Yamasaki, K. Fukao, G. Zhang, T. Kinoshita, K. Mito, H. Hirashima, and K. Sasaki, J. Non-Cryst. Solids **196**, 63 (1996).
[9] K. Tanaka, K. Kashima, K. Hirao, N. Soga, A. Mito, and H. Nasu, Jpn. J. Appl. Phys., Part 2 **32**, L843 (1993).
[10] K. Tanaka, K. Kashima, K. Kajihara, K. Hirao, N. Soga, A. Mito, and H. Nasu, Proc. SPIE **2289**, 167 (1994).
[11] K. Tanaka, K. Kashima, K. Hirao, N. Soga, A. Mito, and H. Nasu, J. Non-Cryst. Solids **185**, 123 (1995).
[12] K. Tanaka, A. Narazaki, K. Hirao, and N. Soga, J. Appl. Phys. **79**, 3798 (1996).
[13] K. Tanaka, A. Narazaki, K. Hirao, and N. Soga, J. Non-Cryst. Solids **203**, 49 (1996).
[14] A. Narazaki, K. Tanaka, K. Hirao, and N. Soga, J. Appl. Phys. **83**, 3986 (1998).
[15] A. Narazaki, K. Tanaka, K. Hirao, and N. Soga, J. Am. Ceram. Soc. **81**, 2735 (1998).
[16] M. J. Redman and J. H. Chen, J. Am. Ceram. Soc. **50**, 523 (1967).
[17] A. A. Appen and G. Fuxi, Fiz. Tverd. Tela (Leningrad) **1**, 1529 (1959).
[18] P. D. Maker, R. W. Terhune, M. Nisenoff, and C. M. Savage, Phys. Rev. Lett. **8**, 21 (1962).
[19] J. Jerphagnon and S. K. Kurtz, J. Appl. Phys. **41**, 1667 (1970).
[20] M. Qiu, F. Pi, G. Orriols, and M. Bibiche, J. Opt. Soc. Am. B **15**, 1362 (1998).
[21] D. E. Carlson, J. Am. Ceram. Soc. **57**, 291 (1974).
[22] D. E. Carlson, K. W. Hang, and G. F. Stockdale, J. Am. Ceram. Soc. **57**, 295 (1974).
[23] A. Berthereau, Y. L. Luyer, R. Olazcuaga, G. L. Flem, M. Couzi, L. Canioni, P. Segonds, L. Sarger, and A. Ducasse, Mater. Res. Bull. **29**, 933 (1994).
[24] T. M. Proctor and P. M. Sutton, J. Chem. Phys. **30**, 212 (1959).
[25] T. M. Proctor and P. M. Sutton, J. Am. Ceram. Soc. **43**, 173 (1960).
[26] R. Terai and R. Hayami, J. Non-Cryst. Solids **18**, 217 (1975).